

ROBUST EXTREMUM SEEKING FOR A SECOND ORDER UNCERTAIN PLANT USING A SLIDING MODE CONTROLLER

CESAR SOLIS ^{a,*}, JULIO CLEMPNER ^b, ALEXANDER POZNYAK ^a

^aCenter for Research and Advanced Studies
 National Polytechnic Institute, Av. Instituto Politécnico Nacional 2508
 Col. San Pedro Zacatenco, Del. Gustavo A. Madero, 07360 Mexico City, Mexico
 e-mail: {csolis, apoznyak}@ctrl.cinvestav.mx

^bSchool of Physics and Mathematics
 National Polytechnic Institute, Av. Instituto Politécnico Nacional, Building 9
 San Pedro Zacatenco, Gustavo A. Madero, 07738 Mexico City, Mexico
 e-mail: julio@clempner.name

This paper suggests a novel continuous-time robust extremum seeking algorithm for an unknown convex function constrained by a dynamical plant with uncertainties. The main idea of the proposed method is to develop a robust closed-loop controller based on sliding modes where the sliding surface takes the trajectory around a zone of the optimal point. We assume that the output of the plant is given by the states and a measure of the function. We show the stability and zone-convergence of the proposed algorithm. In order to validate the proposed method, we present a numerical example.

Keywords: convex optimization, extremum seeking, continuous-time gradient algorithm, dynamical constrained optimization, unknown functions.

1. Introduction

Run-time optimization requires estimation of the gradient. For solving this problem, we consider the synchronous detection method (SDM) proposed by Armstrong (1914). Raju and Rao (2009), Ulusoy *et al.* (2011), as well as Montesinos-García and Martínez-Guerra (2017) employed this concept in communication systems, modulation/demodulation signals and security. Jignesh *et al.* (2013) use the SDM for satellite communications.

In the control and optimization arena, see the work of Nana *et al.* (2012) for robust and optimal controllers, and Liu *et al.* (2015), who presented a real-time control and optimization framework for embedded systems. Related work on building run-time robust optimization framework algorithms and computational procedures has been reported in the literature. In the robust optimization systems area, Apkarian and Tuan (2000) proposed several applications to local and global robust optimization based on an LMI characterization considering additional

algebraic constraints. Dimitrova and Krastanov (2009) considered a nonlinear model of a biological wastewater treatment process, based on two microbial populations and two substrates. Ghadimi and Lan (2012) suggested an optimal algorithm for stochastic strongly convex optimization considering stochastic and probabilistic uncertainties. An application to photovoltaic systems which maximizes the power of the system is given by Bazzi and Krein (2011). Zhang and Ordóñez (2012) set forth a numerical optimization based approach for extremum seeking control. Sahneh *et al.* (2012) introduced a time-varying extremum point optimization algorithm. Cassandras and Lin (2013) presented an optimization approach for multi-agent persistent monitoring systems with performance constraints.

For second order systems, qun Mei (2013) presented an optimal control based on Fourier transform. Wang *et al.* (2014) described an extremum seeking approach with an accelerating convergence parameter. For unknown maps, Mills and Krstic (2015) presented an algorithm to obtain a derivative estimation employing an extremum

*Corresponding author

seeking technique. Also, Sarkar *et al.* (2017) introduced a robust and optimal controller based on sliding modes for event triggered systems. Solis *et al.* (2018b) proposed a continuous-time extremum seeking algorithm with function measurements disturbed by a stochastic noise. Solis *et al.* (2018a) suggested some advances for constrained stochastic static maps optimization, and presented a continuous-time optimization method for an unknown convex function restricted to a dynamic plant with an available output including a stochastic noise (Solis *et al.*, 2019).

To realize an effective on-line optimization, controlling measurable output of an uncertain dynamic plant, the *sliding mode control* (SMC) technique is suggested to be applied in this paper. The advantages of SMC approach being compared with other methods are as follows:

- SMC technique does not require any exact description of the dynamic model of the controlled plant: neither the structure nor exact values of the parameters are required, only some prior upper estimate of the acceleration (\ddot{x}) is used during the controller designing process;
- the right-hand side of the dynamic equation may also include an external bounded-noise perturbations whose effect can be effectively dismissed by the corresponding sliding-mode controller.

For the description of SMC theory, see the works of Bartoszewicz and Leśniewski (2014), Davila and Poznyak (2010), Eichfelder *et al.* (2017), Liu *et al.* (2018) and Poznyak (2018). Perruquetti and Barbot (2002) introduced basic theory and applications on SMC for systems in engineering. Shtessel *et al.* (2014) suggested a theoretical design of controllers and observers based on sliding modes with some practical applications. Shi *et al.* (2006) presented an interesting application of the SMC to stochastic jump systems with repercussions in engineering. Alnejaili *et al.* (2015) and Belkaid *et al.* (2016) showed important applications of SMC to renewable power systems and a solar panel with battery storage.

The *main contributions* of the paper are as follows:

- (i) a continuous-time robust extremum seeking algorithm for a strongly convex functions are suggested;
- (ii) a wide class of unknown function which are twice differentiable with a bounded Hessian is considered;
- (iii) uncertain dynamic systems, which may include bounded uncertainties are admitted to be considered as an optimization instrument;

- (iv) stability analysis is realized and zone-convergence of the proposed algorithm is shown.

In order to validate the contribution of this paper, we developed two numerical examples. The first example is a generic dynamic system, and the second example is a simplified optimal mechanical control system for a solar panel.

The paper is organized as follows. The next section presents the problem formulation. Section 3 suggests the robust extremum seeking algorithm. We proved the stability and the convergence of the proposed method in Section 4. Section 5 presents the numerical examples (generic plant and simplified mechanical control system for a solar panel). Section 6 concludes the paper.

2. Problem formulation

Consider the problem of an approximate extremum seeking of an unknown (but measurable) function by the state variation of a second order dynamic plant, which may contain both bounded uncertainties and disturbances in the description of its model. Formally, it is formulated as follows: Design a control $\mathbf{u} \in \mathbb{R}^n$ based on the system dynamics

$$\begin{cases} \dot{\mathbf{x}}_1 = \mathbf{x}_2, \\ \dot{\mathbf{x}}_2 = g(\mathbf{x}_1, \mathbf{x}_2, t) + \mathbf{u}, \\ y(\cdot) = f(\cdot), \end{cases} \quad (1)$$

which asymptotically tends to a small \varkappa -neighborhood (\varkappa should be estimated) of the extremal point $\mathbf{x}_1^* = \arg_{\mathbf{x}_1 \in \mathbb{R}^n} \min f(\cdot)$ of the optimized function $f: \mathbb{R}^n \rightarrow \mathbb{R}$, namely,

$$\mathbf{x}_1(t) \xrightarrow[t \rightarrow \infty]{} X_\varkappa := \{\mathbf{x}_1 \in \mathbb{R}^n \mid \|\mathbf{x}_1 - \mathbf{x}_1^*\| \leq \varkappa\} \quad (2)$$

with the following assumptions:

1. $\mathbf{x}_1, \mathbf{x}_2 \in \mathbb{R}^n$ the known states of the plant and $\mathbf{u} \in \mathbb{R}^n$ the input control;
2. $g: \mathbb{R}^n \times \mathbb{R}^n \times \mathbb{R} \rightarrow \mathbb{R}^n$ defined by $g(\mathbf{x}_1, \mathbf{x}_2, t)$ is a smooth function that represents the description of the the dynamical plant with nonmodeled uncertainties, which satisfies

$$\|g(\mathbf{x}_1, \mathbf{x}_2, t)\| \leq c_0 + c_1 \|\mathbf{x}_1\| + c_2 \|\mathbf{x}_2\|$$

for some known constants $c_0, c_1, c_2 > 0$;

3. $f: \mathbb{R}^n \rightarrow \mathbb{R}$ is an unknown twice differentiable strongly convex function such that $h_- \mathbb{I} < \nabla^2 f(\mathbf{x}_1) < h_+ \mathbb{I}$ for some known constants $h_+, h_- > 0$,
4. $y(\cdot) \in \mathbb{R}^n$ is a measurable output signal about the aforementioned function.

The problem considers a continuous-time strongly convex unknown function $f(\cdot)$ with bounded dynamical constraints including uncertainties. We shall propose a robust closed-loop controller that stabilizes the system around an optimal convergence zone.

In the next section the method of on-line gradient estimation, will be considered based only on function measurements. The functionality of the suggested robust extrema seeking method will be also discussed.

3. Robust extremum seeking

Let x be a \mathbb{R}^n vector. We define $\text{sign}(x) := [\text{sign}(x_m)]_m$ with $m \in \llbracket 1, n \rrbracket$.

The suggested algorithm to solve the problem (1) is as follows:

$$\begin{cases} \hat{D} = \frac{1}{\alpha} \zeta_t y(\mathbf{x}_1 + \alpha \zeta_t), \\ \dot{\mathbf{J}}_o = \beta (\hat{D} - \mathbf{J}_o) \\ \dot{\mathbf{J}} = \beta (\mathbf{J}_o - \mathbf{J}), \\ \mathbf{u} = -\mu \dot{\mathbf{J}} - U_{\max} [c_0 + c_1 \|\mathbf{x}_1\| \\ + c_2 \|\mathbf{x}_2\|] \text{sign}(\mu \mathbf{J} + \mathbf{x}_2) \end{cases} \quad (3)$$

with the following assumptions:

- (i) constants $\beta, \mu, \alpha > 0$ and $U_{\max} \geq 1$,
- (ii) the auxiliary states $\hat{D}, \mathbf{J}, \mathbf{J}_o \in \mathbb{R}^n$,
- (iii) the dither signal ζ_t is defined as follows:

$$\zeta_t := [\sin(\omega_0 t), \sin(2\omega_0 t), \dots, \sin(n\omega_0 t)]^\top, \quad (4)$$

where $\omega_0 > 0$ is sufficiently large. The dither signal ζ_t is defined as in (4) to satisfy the orthogonality properties of the system and to obtain a correct representation for the time-dependent functions. Figure 1 shows the block structure of the proposed algorithm given in (3).

3.1. Gradient estimation. For simplicity, in this section, we consider the time-dependent vector $x_t := \mathbf{x}_1$ and we introduce the following definition and notation.

Definition 1. (Fourier transform) For a time-dependent integrable real value function $h(t)$, the Fourier transform, denoted by $\overline{h(t)}(\omega)$ in the frequency domain is given by

$$\overline{h(t)}(\omega) := \int_{-\infty}^{\infty} h(t) \exp(-i\omega t) dt. \quad (5)$$

Lemma 1. (Stade, 2005) For an integrable real-valued function $h(t)$ and for some constant $\omega_0 > 0$ we have that

$$\begin{aligned} & \overline{\sin(n\omega_0 t) h(t)}(\omega) \\ &= \frac{1}{2i} \left(\overline{h(t)}(\omega + n\omega_0) - \overline{h(t)}(\omega - n\omega_0) \right), \quad (6) \end{aligned}$$

$$\begin{aligned} & \overline{\sin(n\omega_0 t) \sin(m\omega_0 t) h(t)}(\omega) \\ &= \frac{1}{4} \left(\overline{h(t)}(\omega - (m-n)\omega_0) \right. \\ & \quad + \overline{h(t)}(\omega - (n-m)\omega_0) \\ & \quad - \overline{h(t)}(\omega - (n+m)\omega_0) \\ & \quad \left. - \overline{h(t)}(\omega + (m+n)\omega_0) \right). \quad (7) \end{aligned}$$

In particular, we have that

$$\begin{aligned} & \overline{\sin^2(n\omega_0 t) h(t)}(\omega) \\ &= \frac{1}{2} \overline{h(t)}(\omega) \\ & \quad - \frac{1}{4} \left(\overline{h(t)}(\omega - 2n\omega_0) + \overline{h(t)}(\omega + 2n\omega_0) \right). \quad (8) \end{aligned}$$

Notice that if Eqn. (6) for $\omega_0 > 0$ the spectrum of $h(t)$ is displaced $\pm\omega_0$ around central frequency and in (8) there is a spectral component around the origin. This property will be used to separate the spectrum of the gradient estimation signal from other components.

Definition 2. (Heaviside function) Let us define the complex value Heaviside function as follows:

$$\text{Heaviside}(z) := \begin{cases} 1, & \Re(z) > 0, \\ 0, & \Re(z) \leq 0, \end{cases}$$

where $\Re(z)$ is the real part of $z \in \mathbb{C}$. This definition can be extended to a vector form as follows: let z be a complex vector in \mathbb{C}^n ; then $\text{Heaviside}(z) := [\text{Heaviside}(z_m)]_m$ for every entry $m \in \llbracket 1, n \rrbracket$.

Proposition 1. (Frequency analysis for the estimator) Let x_t be a time-dependent vector in \mathbb{R}^n . Consider a function $f(\cdot)$ given in (1) which admits a Fourier transform given by $\overline{f(\cdot)}(\omega)$. On the above assumptions, let ω_d be the bandwidth of the gradient $\nabla f(\cdot)$. Then for some small $\alpha > 0$ and a sufficiently large dither frequency ω_0 of the dither signal ζ_t , we have that

$$\overline{\frac{1}{\alpha} \zeta_t f(x_t + \alpha \zeta_t)}(\omega) \cdot H(\omega) = \frac{1}{2} \overline{\nabla f(\epsilon_t)}(\omega), \quad (9)$$

where $\epsilon_t = a_t x_t + (1 - a_t)(x_t + \alpha \zeta_t)$ for some $a_t \in [0, 1]$ and

$$H(\omega) := \text{Heaviside}(\omega + \omega_d) - \text{Heaviside}(\omega - \omega_d) \quad (10)$$

with $0 < \omega_d \ll \omega_0$.

Proof. Recall the mean value theorem:

$$f(x_t + \alpha \zeta_t) - f(x_t) = (\alpha \zeta_t)^\top \nabla f(\epsilon_t), \quad (11)$$

where ϵ_t is given as in the formulation of the proposition. Rewriting (11) and pre-multiplying it by $\frac{1}{\alpha} \zeta_t$, we obtain

$$\frac{1}{\alpha} \zeta_t f(x_t + \alpha \zeta_t) = \frac{1}{\alpha} \zeta_t f(x_t) + \zeta_t \zeta_t^\top \nabla f(\epsilon_t).$$

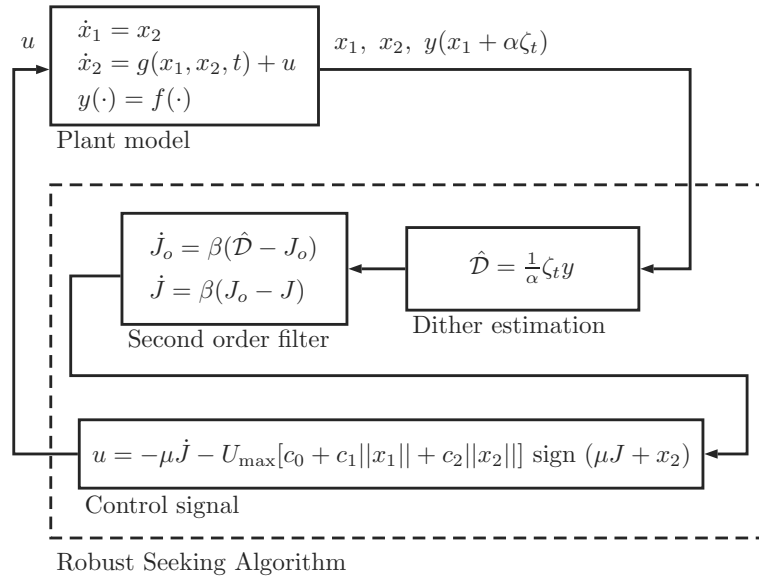


Fig. 1. Block diagram structure for the algorithm.

Apply the Fourier transform:

$$\begin{aligned} \overline{\frac{1}{\alpha} \zeta_t f(x_t + \alpha \zeta_t)}(\omega) &= \frac{1}{\alpha} \overline{\zeta_t f(x_t)}(\omega) + \overline{\zeta_t \zeta_t^T \nabla f(\epsilon_t)}(\omega). \end{aligned}$$

This is an \mathbb{R}^n vector for any entry $m \in \llbracket 1, n \rrbracket$. Then applying (6) to entry m for the first sum we obtain

$$\begin{aligned} \left[\overline{\zeta_t f(x_t)}(\omega) \right]_m &= \frac{1}{2i} \left(\overline{f(x_t)}(\omega + m\omega_0) - \overline{f(x_t)}(\omega - m\omega_0) \right). \end{aligned}$$

For the second sum we apply (7) and (8) to the entry m . From the properties of the matrix multiplication we obtain

$$\begin{aligned} \left[\overline{\zeta_t \zeta_t^T \nabla f(\epsilon_t)}(\omega) \right]_m &= \frac{1}{4} \sum_{j=1}^n \left(\left[\overline{\nabla f(\epsilon_t)}(\omega - (m-j)\omega_0) \right]_j \right. \\ &\quad + \left[\overline{\nabla f(\epsilon_t)}(\omega - (j-m)\omega_0) \right]_j \\ &\quad - \left[\overline{\nabla f(\epsilon_t)}(\omega - (j+m)\omega_0) \right]_j \\ &\quad \left. - \left[\overline{\nabla f(\epsilon_t)}(\omega + (m+j)\omega_0) \right]_j \right). \end{aligned}$$

Consider an ideal low pass filter with a transfer function given by the Heaviside function Eqn. (10) with $\omega_0 \gg \omega_d$. Then the product of this Heaviside function with the Fourier transform yields a cutting frequency resultant and we obtain (9). ■

Remark 1. Observe that (9) represents the frequency spectrum of the gradient $\nabla f(\cdot)$ with some error introduced by ϵ_t . Notice that $H(\omega)$ is a transfer function for an ideal filter implying that it is not realizable. Then, for practical considerations it is important to design a low-pass filter with a flat response and a minimum phase change in the output.

In order to illustrate the previous remark, calculate the Taylor expansion of $f(x_t + \alpha \zeta_t)$. Taking into account (9), after some algebra we have that

$$\nabla f(\epsilon_t) = \nabla f(x_t) + o(\alpha^2).$$

Now, consider the realizable second order filter given by

$$\begin{cases} \dot{\mathbf{J}}_o = \beta (\hat{\mathcal{D}} - \mathbf{J}_o), \\ \dot{\mathbf{J}} = \beta (\mathbf{J}_o - \mathbf{J}). \end{cases} \quad (12)$$

It is possible to analyze every entry as a transfer function as follows:

$$\frac{[\mathbf{J}]_m}{[\hat{\mathcal{D}}]_m} = \frac{1}{\left(\frac{1}{\beta}i\omega + 1\right)^2}.$$

Then we have that

$$[\mathbf{J}]_m = \frac{\left[\frac{1}{\alpha} \zeta f(x_t + \alpha \zeta_t) \right]_m(\omega)}{\left(\frac{1}{\beta}i\omega + 1\right)^2}.$$

Clearly, it is not possible to obtain an analytic inverse of the Fourier transform. However, we can consider the limit points to approximate the expression. Then, remembering

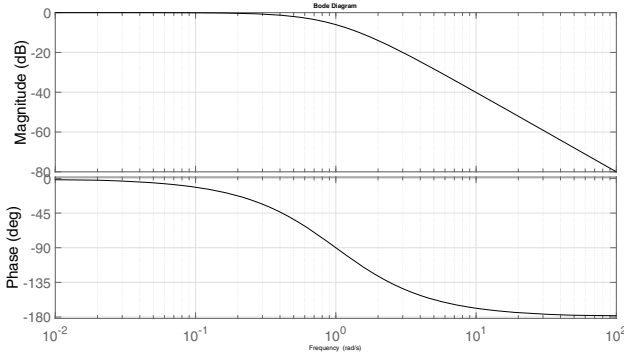


Fig. 2. Bode diagram design.

that $\nabla f(\cdot)$ is a limited bandwidth ω_d , it is possible to choose $\beta > 0$ such that for $\omega \geq 0$,

$$[\mathbf{J}]_m \approx \begin{cases} \frac{1}{\alpha} \zeta_t f(x_t + \alpha \zeta_t)(\omega) \\ \cdot H(\omega), & \omega \leq \omega_d \ll \beta \ll \omega_0, \\ 0, & \omega \gg \beta, \end{cases}$$

Figure 2 illustrates a method to tune the filter, where β is the cutting angular frequency. For practical purposes it is common to use $\beta = 10\omega_d = 0.1\omega_0$. It is possible to design high order filters different from the proposed filter, but the delay group time increases implying a general delay in the global system. Then the output of the filter is as follows:

$$\mathbf{J} = \nabla f(x_t) + o(\alpha^2). \quad (13)$$

3.2. Proof of stability and of convergence.

Lemma 2. (Surface stability) *With the assumptions and notation given in (1) and (3) the dynamics $\dot{\mathbf{x}}_1 = -\mu\mathbf{J}$ is stable in a \varkappa -zone around the optimal point \mathbf{x}_1^* , that is,*

$$\limsup_{t \rightarrow \infty} \|\mathbf{x}_1^* - \mathbf{x}_1(t)\| \leq \varkappa := \frac{h_+}{h_-^2} |o(\alpha^2)|. \quad (14)$$

Proof. For notational simplicity we employ the following symbols:

$$\mathcal{D} := \nabla f(\mathbf{x}_1),$$

$$\mathcal{H} := \nabla^2 f(\mathbf{x}_1).$$

Consider the Lyapunov function

$$V := \mathcal{D}^\top \mathcal{D}.$$

Taking the time-derivative, we get

$$\dot{V} = 2\mathcal{D}^\top \mathcal{H} \dot{\mathbf{x}}_1 = -2\mu \mathcal{D}^\top \mathcal{H} \mathbf{J}$$

and in view of $\mathbf{J} = \mathcal{D} + o(\alpha^2)$ and by Eqn. (13) we have

$$\begin{aligned} \dot{V} &= -2\mu \mathcal{D}^\top \mathcal{H} \mathcal{D} - 2\mu \mathcal{D}^\top \mathcal{H} o(\alpha^2) \\ &\leq -2\mu h_- \|\mathcal{D}\|^2 + 2\mu h_+ \|\mathcal{D}\| |o(\alpha^2)|. \end{aligned}$$

For some $\epsilon > 0$ (by Λ -inequality)

$$\begin{aligned} \dot{V} &\leq -2\mu h_- \|\mathcal{D}\|^2 + \mu h_+ (\epsilon \|\mathcal{D}\|^2 + \epsilon^{-1} |o(\alpha^4)|) \\ &= -\mu \|\mathcal{D}\|^2 (2h_- - h_+ \epsilon) + \mu h_+ \epsilon^{-1} |o(\alpha^4)|. \end{aligned}$$

Then, choosing $0 < \epsilon < 2h_-/h_+$ and renaming $\rho := \mu(2h_- - h_+ \epsilon)$ and $\epsilon_0 := \mu h_+ \epsilon^{-1} |o(\alpha^4)|$, we have that

$$\dot{V} \leq -\rho V + \epsilon_0, \quad (15)$$

implying

$$\limsup_{t \rightarrow \infty} V \leq \frac{\epsilon_0}{\rho} = \frac{h_+ |o(\alpha^4)|}{(2h_- - h_+ \epsilon) \epsilon}.$$

Notice that if we select $\epsilon = h_-/h_+$, we obtain the following minimum bound:

$$\limsup_{t \rightarrow \infty} V \leq \frac{h_+^2}{h_-^2} |o(\alpha^4)|.$$

Returning to the original notation, this implies

$$\limsup_{t \rightarrow \infty} \|\nabla f(\mathbf{x}_1)\| \leq \frac{h_+}{h_-} |o(\alpha^2)|.$$

Applying Cauchy's mean value theorem to the gradient and taking account of the fact that $\nabla f(\mathbf{x}_1^*) = 0$, we have

$$\nabla f(\mathbf{x}_1) = \nabla^2 f((c-1)\mathbf{x}_1 + c\mathbf{x}_1^*)(\mathbf{x}_1^* - \mathbf{x}_1),$$

where $c \in [0, 1]$. Majoring by taking the norm and the assumptions for $f(\cdot)$ yields (14). This completes the proof. ■

Remark 2. The following facts are easy to check:

- (i) Substituting the value ϵ in ρ , we obtain $\rho = \mu h_-$ ($\mu > 0$) which controls the speed of convergence. Now, for (15) it is possible to solve the inequality

$$V(t) \leq \frac{\epsilon_0}{\mu h_-} + V(0) \exp(-\mu h_- t).$$

- (ii) If we choose a very small parameter $\alpha > 0$, it is possible to guarantee the convergence to a small zone. It is important to note that the term $\hat{\mathcal{D}}$ can present an undesirable numerical singularity.

Theorem 1. (Global stability and convergence) *Under the above assumptions the optimal seeking algorithm given in (3) applied to the problem (1) satisfies the following:*

- (i) the dynamics $\sigma := \mu\mathbf{J} + \mathbf{x}_2 = 0$ is stable,

(ii) the global system reaches the sliding surface $\sigma = 0$ in finite time,

(iii) the global system is stable and converges to a zone around the optimal point.

Proof. Let us consider the sliding surface $\sigma \in \mathbb{R}^n$ such that

$$\sigma := \mu \mathbf{J} + \mathbf{x}_2 = 0. \tag{16}$$

By (1) and Lemma 2 we have that $\sigma = \mu \mathbf{J} + \dot{\mathbf{x}}_1$, which is a stable surface, proving (i). Then, we can apply sliding mode control theory to the problem. Considering a Lyapunov-like function of the form

$$\mathcal{V}(t) = \frac{1}{2} \sigma^T \sigma$$

and taking its time-derivative we have that

$$\begin{aligned} \dot{\mathcal{V}}(t) &= \sigma^T \dot{\sigma} \\ &= \sigma^T [\mu \dot{\mathbf{J}} + g(\mathbf{x}_1, \mathbf{x}_2, t) + \mathbf{u}]. \end{aligned} \tag{17}$$

Select the control as $\mathbf{u} := -\mu \dot{\mathbf{J}} + \mathbf{u}_0$. Suppose that for $[\sigma]_m < 0$ we need $[\mathbf{u}_0]_m > \|[g(\mathbf{x}_1, \mathbf{x}_2, t)]_m\|$ and for $[\sigma]_m > 0$ we need $[\mathbf{u}_0]_m < -\|[g(\mathbf{x}_1, \mathbf{x}_2, t)]_m\|$, but

$$\begin{aligned} \|[g(\mathbf{x}_1, \mathbf{x}_2, t)]_m\| &\leq \|g(\mathbf{x}_1, \mathbf{x}_2, t)\| \\ &\leq c_0 + c_1 \|\mathbf{x}_1\| + c_2 \|\mathbf{x}_2\|. \end{aligned}$$

Then, choose the control law \mathbf{u}_0 as follows:

$$\mathbf{u}_0 = -U_{\max} [c_0 + c_1 \|\mathbf{x}_1\| + c_2 \|\mathbf{x}_2\|] \text{sign}(\sigma)$$

for some $U_{\max} \geq 1$. Hence, the control signal is given by

$$\begin{aligned} \mathbf{u} &:= -\mu \dot{\mathbf{J}} - U_{\max} [c_0 + c_1 \|\mathbf{x}_1\| + c_2 \|\mathbf{x}_2\|] \\ &\quad \times \text{sign}(\mu \mathbf{J} + \mathbf{x}_2). \end{aligned} \tag{18}$$

Substituting this result in (17) and applying the triangle inequality, we get

$$\dot{\mathcal{V}}(t) \leq -U_{\max} |\sigma| = -U_{\max} \sqrt{2\mathcal{V}(t)}.$$

Now, by solving the ordinary differential inequality, the reaching time to the sliding surface is bounded by

$$t_{\text{reach}} \leq \frac{1 + \sqrt{U_{\max}(U_{\max} - 1)}}{U_{\max}} \sqrt{2\mathcal{V}(0)}$$

proving (ii).

When the sliding surface is reached, the behavior of the global system is given by the dynamics $\dot{\mathbf{x}}_1 = -\mu \mathbf{J}$ and by Lemma 2 it is possible to conclude (iii). ■

Remark 3. (*Practical selection of the parameters*) In Sections 3 and 4 we present the theoretical background of the real-time optimal algorithm under conditions and constraints presented in Section 2. In order to select the parameters, we suggest the following:

1. Verify that the global plant satisfies approximately the conditions given in Section 2.
2. Try to stabilize the plant choosing $0 < \alpha < 1$, $0 < \beta < 10$, $0 < \mu < 2$, $1 < U_{\max} < 2$, and $0 < c_0$, $0 < c_1$ and $0 < c_2$.
3. If the plant is stable then reduce the values for c_0 , c_1 and c_2 to decrease the input control signal, otherwise increase these values.
4. To decrease the time of convergence, increase the values $0 < \mu$ and $1 < U_{\max}$ such that the actuators and the global system plant allows it.
5. To obtain the best convergence zone decrease the values $0 < \alpha$ and $0 < \beta$ taking care of avoiding saturation of the numerical error given by $1/\alpha$ in the algorithm.

The next section demonstrates the effectiveness of the suggested technique being applied to two examples: one is a simple benchmark example and another deals with the control of a solar panel.

4. Numerical examples

4.1. Example 1: A generic plant. Consider the plant given by

$$\begin{cases} \dot{x}_1 = x_2, \\ \dot{x}_2 = \eta(t) + x_2 + \frac{x_1}{1+x_1} + u, \\ y(x_1) = \cosh\left(\frac{1}{5}(x_1 - 15)\right), \end{cases} \tag{19}$$

where $\eta(t) := \sin(t)$ is the disturbance in the state. Note that

$$\begin{aligned} |g(x_1, x_2, t)| &= \left| \eta(t) + x_2 + \frac{x_1}{1+x_1} \right| \\ &\leq 1 + |x_1| + |x_2|. \end{aligned}$$

Then for our algorithm we select the following parameters: $\alpha = 0.1$, $\beta = 10\pi$, $\omega_0 = 1000\pi$, $\mu = 3$, $c_0, c_1, c_2 = 1$, $U_{\max} = 1.5$.

The optimal point is $x_1^* = 15$. Figure 3 show the convergence of the state to the optimal point. The optimization of the functional is presented in Fig. 4. Finally, Figs. 5 and 6 show the control signal and the reached sliding surface, respectively.

4.2. Example 2: A simplified mechanical control system for a solar panel. Consider the problem of tracking the position of the sun in order to expose a simple solar panel to a maximum radiation at a given time. The main goal of a solar tracking system is to obtain the best solar panel orientation at a given time of the day. The solar

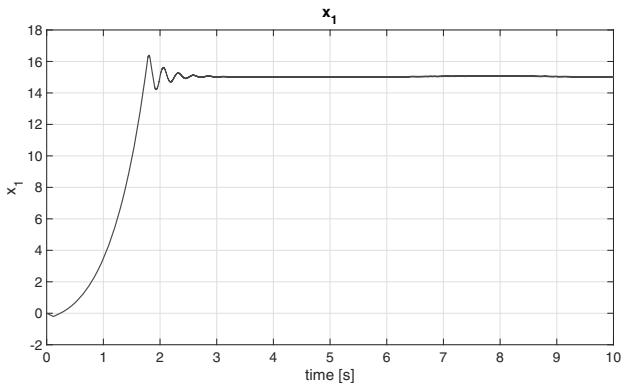


Fig. 3. State $x(t)$.

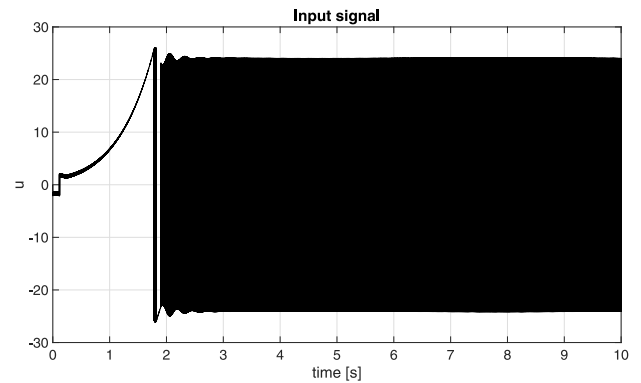


Fig. 5. Control signal.

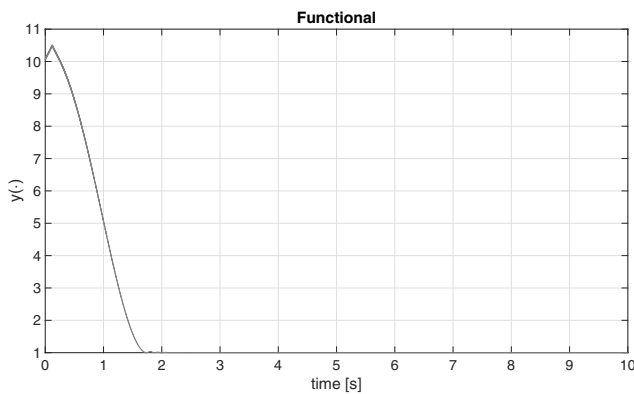


Fig. 4. Optimization of the functional $f(\cdot)$.

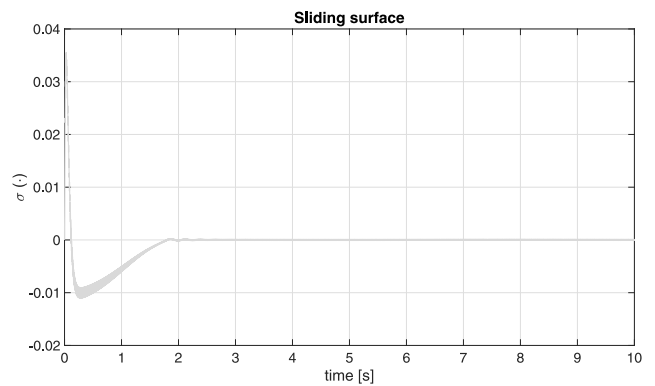


Fig. 6. Sliding surface.

panel is represented in Fig. 7 and its simplified dynamical system given by

$$\begin{cases} I\ddot{\theta} + k\dot{\theta} = \tau + \tau_\eta, \\ y(\cdot) = v_1 \cdot v_2, \end{cases} \quad (20)$$

where I is the rotational inertia of the solar panel, k a viscous friction of the rotor, τ the motor torque, τ_η a disturbance torque over the solar panel, θ the angle from the horizontal plane, v_1 and v_2 are unitary vectors as in the figure. Clearly $y(\cdot)$ is a dot product of two unitary vectors. Then the minimum is -1 when the vectors are oriented in opposite directions, that is, the maximum light intensity. Note that

$$|g(x_1, x_2, t)| = \left| -\frac{k}{I}x_2 + \frac{1}{I}\tau_\eta \right| \leq \frac{1}{I}\tau_\eta + \frac{k}{I}|x_2|.$$

For simulation we choose $I = 5, k = 0.5, \tau_\eta = 1$.

Choosing the parameters $\alpha = 0.1, \beta = 1/2, \omega = 200, \mu = 10, c_0 = 1, c_1 = 0, c_2 = 1$ y $U_{\max} = 1.5$, we can see that the functional tends to the minimum. In Fig. 9 it is possible to see the real-time optimization of

the function, that is, the solar panel tends to follow the maximum of the light. In Fig. 8 we emphasize the turning around to the optimal angle of the solar panel. Finally, Fig. 11 shows the reached sliding surface.

5. Conclusions

This paper presented a new continuous-time robust extremum seeking algorithm for strongly unknown (Hessian bounded) convex functionals constrained by dynamic plants with bounded uncertainties. The outputs of the plant are given by the states of the dynamical and a measure of the functional. The mathematical analysis of the stability and convergence of the method was presented. The main advantages of the suggested approach being compared with other methods are the following:

- it does not require any exact description of the dynamic model of the controlled plant: neither the structure nor exact values of the parameters are required; only some a priori upper estimate of the acceleration are used during the controller design

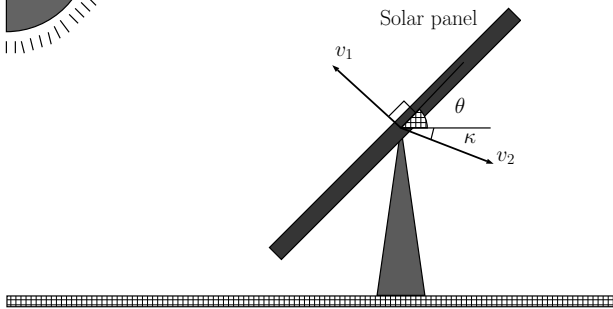


Fig. 7. Solar panel.

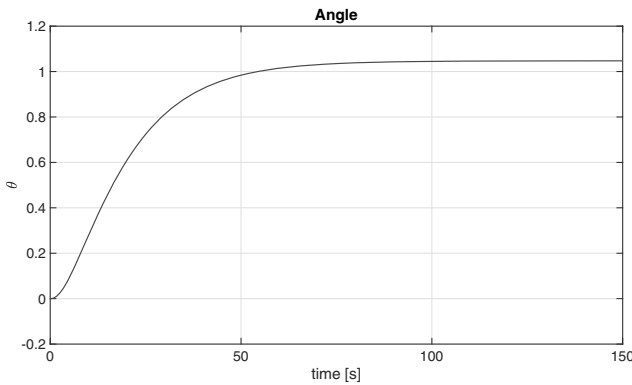


Fig. 8. Angle θ of the solar panel.

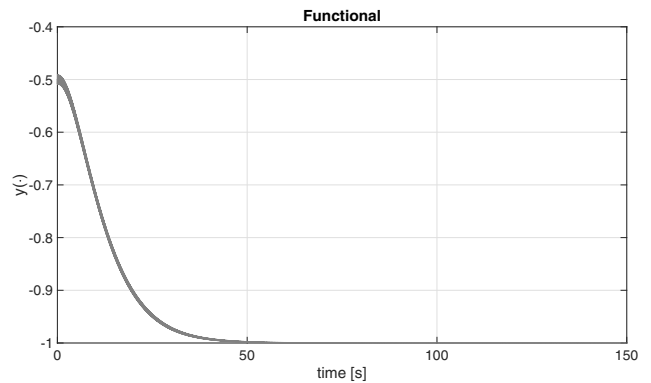


Fig. 9. Functional minimization.

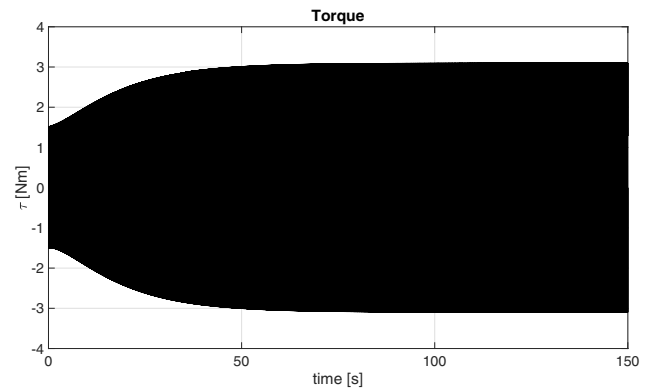


Fig. 10. Motor torque.

process;

- the right-hand side of the dynamic equation *may also include an external bounded noise-perturbations* whose impact can be effectively dismissed by the suggested sliding-mode based controller.

To validate the theoretical background, we presented two numerical examples: (a) the first example consists in a stabilization and optimization of a generic plant considering a strongly convex functional, and (b) the second example applied to a mechanical optimization problem which tracks the position of the sun in order to expose a solar panel to maximum radiation at any given time. Both examples exhibited an optimal real-time behavior. As a future work, we consider improving this algorithm by including algebraic convex constraints and stochastic noise.

References

Alnejaili, T., Drid, S., Mehdi, D., Chrifi-Alaoui, L. and Sahraoui, H. (2015). Sliding mode control of a multi-source renewable power system, *3rd International Conference on*

Control Engineering Information Technology, Tlemcen, Algeria, pp. 1–6.

Apkarian, P. and Tuan, H.D. (2000). Robust control via concave minimization local and global algorithms, *Transactions on Automatic Control* **45**(2): 299–305.

Armstrong, E.H. (1914). Operating features of the audion, *Electrical World* (December 12): 1149–1152.

Bartoszewicz, A. and Leńniewski, P. (2014). An optimal sliding mode congestion controller for connection-oriented communication networks with lossy links, *International Journal of Applied Mathematics and Computer Science* **24**(1): 87–97, DOI: 10.2478/amcs-2014-0007.

Bazzi, A.M. and Krein, P.T. (2011). Concerning “Maximum power point tracking for photovoltaic optimization using ripple-based extremum seeking control”, *IEEE Transactions on Power Electronics* **26**(6): 1611–1612.

Belkaid, A., Colak, I. and Kayisli, K. (2016). Optimum control strategy based on an equivalent sliding mode for solar systems with battery storage, *IEEE International Conference on Power Electronics and Motion Control (PEMC), Varna, Bulgaria*, pp. 1262–1268.

Cassandras, C.G. and Lin, X. (2013). Optimal control of multi-agent persistent monitoring systems with

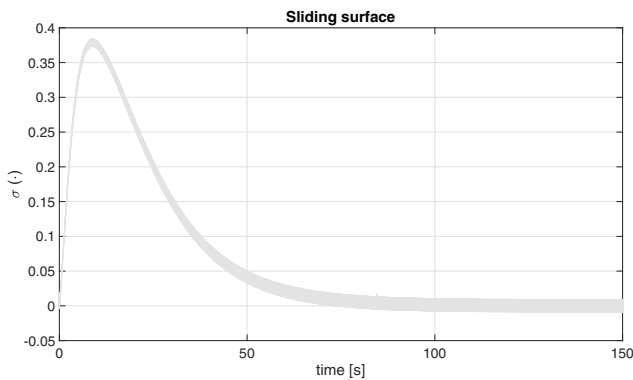


Fig. 11. Sliding surface convergence.

performance constraints, in D.C. Tarraf (Ed.), *Control of Cyber-Physical Systems*, Lecture Notes in Control and Information Sciences, Vol. 449, Springer, Cham, pp. 281–299.

- Davila, J. and Poznyak, A. (2010). Attracting ellipsoid method application to designing of sliding mode controllers, *11th International Workshop on Variable Structure Systems (VSS)*, Mexico City, Mexico, pp. 83–88.
- Dimitrova, N. and Krastanov, M. (2009). Nonlinear stabilizing control of an uncertain bioprocess model, *International Journal of Applied Mathematics and Computer Science* **19**(3): 441–454, DOI: 10.2478/v10006-009-0036-0.
- Eichfelder, G., Krüger, C. and Schöbel, A. (2017). Decision uncertainty in multiobjective optimization, *Journal of Global Optimization* **69**(2): 485–510.
- Ghadimi, S. and Lan, G. (2012). Optimal stochastic approximation algorithms for strongly convex stochastic composite optimization. I: A generic algorithmic framework, *SIAM Journal on Optimization* **22**(4): 1469–1492.
- Jignesh, D.J., Sripati, U. and Kulkarni, M. (2013). Performance of QPSK modulation for FSO geo-synchronous satellite communication link under atmospheric turbulence, *International Conference Emerging Research Areas, Kanjirapally, India*, pp. 1–5.
- Liu, X., Chen, X. and Kong, F. (2015). *Utilization Control and Optimization of Real-Time Embedded Systems*, <https://ieeexplore.ieee.org/document/8187024>.
- Liu, X., Hu, F. and Su, X. (2018). Sliding mode control of a class of nonlinear systems, *7th IEEE Conference on Data Driven Control and Learning Systems (DDCLS)*, Hubei, China, pp. 1069–1072.
- Mills, G. and Krstic, M. (2015). Maximizing higher derivatives of unknown maps with extremum seeking, *54th IEEE Conference on Decision and Control (CDC)*, Osaka, Japan, pp. 5648–5653.
- Montesinos-García, J.J. and Martínez-Guerra, R. (2017). A fractional exponential polynomial state observer in secure communications, *14th International Conference on Electrical Engineering, Mexico, Mexico*, pp. 1–6.
- Nana, S., Yugang, N. and Bei, C. (2012). Optimal integral sliding mode for uncertain discrete time systems, *31st Chinese Control Conference, Hefei, China*, pp. 3155–3159.
- Perruquetti, W. and Barbot, J.P. (2002). *Sliding Mode Control in Engineering*, M. Dekker, New York, NY.
- Poznyak, A. (2018). Stochastic super-twist sliding mode controller, *IEEE Transactions on Automatic Control* **63**(5): 1538–1544.
- qun Mei, W. (2013). Optimal control algorithm of multivariate second-order distributed parameter systems based on Fourier transform, *25th Chinese Control and Decision Conference (CCDC)*, Guiyang, China, pp. 4623–4627.
- Raju, B.V.S.S.N. and Rao, K.D. (2009). Blind robust multiuser detection in synchronous chaotic modulation systems, *Annual IEEE India Conference, Gujarat, India*, pp. 1–4.
- Sahneh, F.D., Hu, G. and Xie, L. (2012). Extremum seeking control for systems with time-varying extremum, *31st Chinese Control Conference, Hefei, China*, pp. 225–231.
- Sarkar, M.K., Arkdev and Singh, S.S.K. (2017). Sliding mode control: A higher order and event triggered based approach for nonlinear uncertain systems, *8th Annual Industrial Automation and Electromechanical Engineering Conference (IEMECON)*, Bangkok, Thailand, pp. 208–211.
- Shi, P., Xia, Y., Liu, G. and Rees, D. (2006). On designing of sliding-mode control for stochastic jump systems, *IEEE Transactions on Automatic Control* **51**(1): 97–103.
- Shtessel, Y., Edwards, C., Fridman, L. and Levant, A. (2014). *Birkhäuser Basel*, Springer Science+Business Media, New York, NY.
- Solis, C., Clempner, J.B. and Poznyak, A.S. (2019). Extremum seeking by a dynamic plant using mixed integral sliding mode controller with stochastic synchronous detection gradient estimation, *International Journal of Robust and Nonlinear Control* **29**(3): 702–714, DOI: 10.1002/rnc.4408.
- Solis, C.U., Clempner, J.B. and Poznyak, A.S. (2018a). Constrained extremum seeking with function measurements disturbed by stochastic noise, *15th International Conference on Electrical Engineering, Mexico City, Mexico*, pp. 1–4.
- Solis, C.U., Clempner, J.B. and Poznyak, A.S. (2018b). Continuous-time extremum seeking with function measurements disturbed by stochastic noise: A synchronous detection approach, *15th International Conference Electrical Engineering, Mexico City, Mexico*, pp. 1–5.
- Stade, E. (2005). *Fourier Analysis*, Wiley-Interscience, Hoboken, NJ.
- Ulusoy, A., Liu, G., Trasser, A. and Schumacher, H. (2011). An analog synchronous QPSK demodulator for ultra-high rate wireless communications, *German Microwave Conference (GeMiC)*, Darmstadt, Germany, pp. 1–4.
- Wang, L., Chen, S. and Zhao, H. (2014). A novel fast extremum seeking scheme without steady-state oscillation, *33rd Chinese Control Conference, Nanjing, China*, pp. 8687–8692.

Zhang, C. and Ordóñez, R. (2012). *Extremum-seeking Control and Applications*, Springer, London.

Cesar U. Solis holds an MSc degree from the Department of Control Automatics at the Center for Research and Advanced Studies (CINVESTAV-IPN), Mexico. He received his BSc in electronics engineering from Metropolitan Autonomous University, Mexico. His research is focused on control theory. He is currently a PhD student in the Department of Control Automatics at the Center for Research and Advanced Studies, majoring in control theory.

Julio B. Clempner holds a PhD in computer science from the Center for Computing Research at National Polytechnic Institute. Dr. Clempner's research interests are focused on game theory and economics. One stream of research is the use of Markov decision processes. A second stream is optimization using extremum seeking. A third stream is employing Petri nets. The final stream is related to optimization and Markov chains. He is currently with Escuela Superior de Física y Matemáticas, Instituto Politécnico Nacional, and is a member of the Mexican National System of Researchers (SNI) as well as a number of North American and European professional organizations. He is also on editorial boards of several journals.

Alexander S. Poznyak graduated from Moscow Physical Technical Institute (MPhTI) in 1970. He earned his PhD and DSc degrees from the Institute of Control Sciences of the Russian Academy of Sciences in 1978 and 1989, respectively. From 1973 up to 1993 he served at this institute as a researcher and a leading researcher, and in 1993 he accepted the post of a full professor (3-F) at CINVESTAV of IPN in Mexico. At present, he is the head of the Automatic Control Department. He has published more than 200 papers in various international journals and 10 books. He is a regular member of the Mexican Academy of Sciences and the System of National Investigators (SNI -3). He is also a fellow of the IMA.

Received: 30 November 2018

Revised: 18 April 2019

Accepted: 19 July 2019